World Academy of Science, Engineering and Technology
International Journal of Geological and Environmental Engineering
Vol:17, No:3, 2023

Effect of Sand Particle Transportation in Oil and Gas Pipeline Erosion

Christopher Deekia Nwimae, Nigel Simms, Liyun Lao

***Abstract*—**Erosion in a pipe bends caused by particles is a major concern in the oil and gas fields and might cause breakdown to production equipment. This work investigates the effect of sand particle transport in an elbow using computational fluid dynamics (CFD) approach. Two-way coupled Euler-Lagrange and discrete phase model is employed to calculate the air/solid particle flow in the elbow. Generic erosion model in Ansys fluent and three particle rebound models are used to predict the erosion rate on the 90° elbows. The model result is compared with experimental data from the open literature validating the CFD-based predictions which reveals that due to the sand particles impinging on the wall of the elbow at high velocity, a point on the pipe elbow were observed to have started turning red due to velocity increase and the maximum erosion locations occur at 48°.

***Keywords*—**Erosion, prediction, elbow, computational fluid dynamics, CFD.

I. Introduction

SAND production in oil and gas pipeline is a significant concern to the industry, which may jeopardise equipment performance leading to failure. As a prevalent component in pipeline infrastructure, 90°elbows are used to change flow direction in pipelines. Rapid deviation in direction of flow can produce huge change in distribution of sand particles. Reference [1] has shown that erosion on a pipeline with high pressure usually occur in an elbow and the mass loss rate due to particle impingement may be fifty times higher than mass loss in straight pipe [1]. In recent time, numerous erosion mechanism and theoretical model have been recommended [2]; an equation for erosional calculation of elbow was given by American Petroleum Institute (API-14E) criterion which examines particle velocity and quantities, [3] and [4] examine material density and recommended a method for erosion rate calculation. Reference [5] recommended a modify equation for calculating erosion rate on particle size and mixture density. Reference [6] consider the flow field during computing of particle erosion in air and water flow, and [7] suggested a technique to assess erosion rate in multiphase flow which is centred on numerical simulation and mechanistic evaluation. Therefore, it is essential to obtain an effective method of predicting the erosion distribution around an elbow which is important for the integrity of pipeline management. Furthermore, the accurate prediction of erosion rate makes it simpler to find erosion hotspot and allow for the evaluation of service life of pipe. A lot of experimental work has been done previously to investigate particle erosion in elbows [8]-[12]; most of the experiments were conducted to examine the maximum erosion rate of an elbow and the continuous erosion profile about the elbow. This paper will address the use of a CFD methodology to predict the location of erosion hotspots in a 90º elbow. The Eulerian-Lagrangian approach for continuous and discrete phase calculations with different turbulence models has been implemented to investigate the importance of erosion mechanisms in pipe elbows.

II. Simulation

A. Modelling

Three main steps in CFD-based erosion modelling are: the continuous phase simulation flow field, tracking of particle and calculation of erosion rate. In present work, the fluid phase is treated as a continuous phase and is solved by the Navier-Stokes governing equation. The sand particles are treated as discrete phase and are solved by Newton's second law motion. In addition, two-way coupling is employed between the continuous phase and discrete phase.

B. The Continuous Phase Models

The Navier-Stokes equations are employed here. The general equations of continuity and momentum are given as:

$$\frac{\partial \rho}{\partial t} + \nabla(\rho \vec{u}) = 0 \tag{1}$$

$$\frac{\partial}{\partial t}(\rho \vec{u}) + \nabla \cdot (\rho \vec{u}\ \vec{u}) = -\nabla P + \nabla \cdot (\bar{\bar{\tau}}) + \rho \vec{g} + \vec{S} m \tag{2}$$

where ρ is fluid density, $\vec{u}$ is instantaneous velocity vector of fluid, P is the static pressure, $\bar{\bar{\tau}}$ is the stress tensor, $\rho \vec{g}$ is the body force, $\vec{S}$M is the additional momentum due to discrete phase. The stress tensor is given as:

$$\bar{\bar{\tau}} = \mu \left[(\nabla \vec{u} + \nabla \vec{u}^{T}) - \frac{2}{3} \nabla \cdot \vec{u} I \right] \tag{3}$$

where μ is viscosity of fluid, I is unit tensor. The turbulence model standard k-omega-shear stress transport (SST) is used in this work to calculate the flow turbulence, equations are given as:

Christopher Deekia Nwimae is a PhD researcher in Cranfield University, Bedfordshire, MK43 0AL, United Kingdom (phone: +44(0)7721807828; e-mail: Christopher.d.nwimae@cranfield.ac.uk).

Professor Nigel Simms, Energy and Power Theme, Cranfield University, Bedfordshire, MK43 0AL, United Kingdom (phone: +44 (0) 123475295; e-mail: n.j.simms@cranfield.ac.uk).

Dr Liyun Lao, Principal Research Fellow, Energy and Power Theme, Cranfield University, Bedfordshire, MK43 0AL, United Kingdom (phone: +44 (0) 1234758266; e-mail: l.lao@cranfield.ac.uk).

$$\frac{\partial(\rho k)}{\partial t}+\frac{\partial(\rho k u i)}{\partial x i}=\frac{\partial}{\partial x j}\left[\left(\mu+\frac{\mu t}{\sigma k}\right)\frac{\partial k}{\partial x j}\right]+G_k-\rho\varepsilon+S_k \quad (4)$$

$$\frac{\partial(\rho\varepsilon)}{\partial t}+\frac{\partial(\rho\varepsilon u i)}{\partial x i}=\frac{\partial}{\partial x i}\left[\left(\mu+\frac{\mu t}{\sigma\varepsilon}\right)\frac{\partial\varepsilon}{\partial x i}\right]+C_{1\varepsilon}\frac{\varepsilon}{k}G_k-C_{2\varepsilon}\rho\frac{\varepsilon^2}{k}+S_\varepsilon \quad (5)$$

where G_k is the generation of turbulence kinetic energy due to mean velocity gradients, u_i is the velocity component in the i direction, x_i and x_j are the spatial coordinates, σ_k and σ_ε are turbulent Prandtl numbers for k and ε, $C_{1\varepsilon}$ and $C_{2\varepsilon}$ are constants, S_k and S_ε are source terms, $\mu_t=\rho C_\mu\frac{k^2}{\varepsilon}, \sigma_k=1.0, \sigma_\varepsilon=1.3, C_{1\varepsilon}=1.44, C_{2\varepsilon}=1.92, C_\mu=0.09$.

C. Discrete/Dispersed Phase Model

The discrete/dispersed phase model is employed, in which particle trajectories are acquired by integrating the motion equation of particles under the Lagrangian coordinates. The governing equation of particle motion of the fluid according to Newton's second law is:

$$\frac{d\vec{u}p}{dt}pm=\overrightarrow{F}_D+\overrightarrow{F}_P+\overrightarrow{F}_B+\overrightarrow{F}_c \quad (6)$$

From the first term on the right hand to the last term of (6): $\vec{F}_D$ denotes drag force, $\vec{F}_P$ pressure gradient force, $\vec{F}_M$ mass force and $\vec{F}_{BG}$ buoyancy force. The main hydrodynamic force that acts on particles is the drag force:

$$\overrightarrow{F}_D=\frac{18\mu}{\rho_P d_p^2}\frac{C_d Re_p}{24}\left(\overrightarrow{u}-\overrightarrow{u_p}\right) \quad (7)$$

where $\overrightarrow{u}\rho$ is particle velocity vector, d_p is particle diameter, ρ_p is density of particles, Re_p is particle Reynolds number:

$$Re_p=\frac{\rho d_p\left|\overrightarrow{u_p}-\vec{u}\right|}{\mu} \quad (8)$$

C_d the coefficient of drag

$$C_d=a_1+\frac{a_2}{Re_p}+\frac{a_3}{Re_p^2} \quad (9)$$

where a_1, a_2, a_3 are constants for smooth spherical particles, and the three particle parameters differs with the Reynolds number. The pressure gradient force is caused by the pressure change in the flow

$$\overrightarrow{F}_P=\left(\frac{\rho}{\rho_p}\right)\nabla P \quad (10)$$

The virtual mass force is given as:

$$\overrightarrow{F}_B=\frac{1}{2}\frac{\rho d(\overrightarrow{u}-\overrightarrow{u_p})}{\rho_p dt} \quad (11)$$

The buoyancy force is given as:

$$\overrightarrow{F}_A=\frac{(\rho_p-\rho)}{\rho_p}\overrightarrow{g} \quad (12)$$

In this work the particles are small, pressure change over distance of particle diameter is negligible. Consequently, the density of fluid is much lower than the density of the particles, the pressure gradient force can be neglected. As the virtual mass force is important only when the fluid density is larger than the particles density, the virtual mass force can also be neglected.

D.Mechanism of Coupling between Two Phases

To achieve precise particle trajectories and erosion distributions, the coupling of continuous phase and the dispersed phase need to be considered, especially in the conditions that the particle mass loading rate is high or the particle collision is intense.

E. Coupling of Momentum

The momentum exchange is computed by examining the change of the particle momentum when it passes through each control volume, which is expressed as

$$S_M=\sum(F_D+F_A)M_P\nabla t \quad (13)$$

where M_p is referred to as mass flow rate of particles, ∇t is referred to as the time step.

F. Coupling of Turbulence

Stochastic is a tracking method used to predict the effect of turbulent flow fluctuations on particle trajectories. The dispersion of particles in the fluid phase turbulence is calculated using discrete random walk (DRW) model, which uses the instantaneous fluid velocity to incorporate the trajectory given by:

$$u=\bar{u}+u'(t) \quad (14)$$

The turbulent fluctuating velocity that retains Gaussian probability distribution is as follows:

$$u'=\varsigma\sqrt{\overline{u'^2}} \quad (15)$$

where ς referred to random number which obeys normal distribution. And if the local turbulence is isotropic, then the local root mean square (RMS) value of the velocity fluctuation is calculated by:

$$\sqrt{\overline{u'^2}}=\sqrt{\frac{2k}{3}} \quad (16)$$

Production of turbulent eddies causes particle damping and this turbulence eddies can alter the turbulent quantities. Equations (4) and (5) added particle source terms effect into account and the fluid phase turbulent kinetic energy has been modified by the formulation expressed in [9] and [10].

III. Particle-Particle-Wall/Restitution Coefficient Behavior

In CFD code, particle-wall restitution coefficient rebound model is used with erosion model to predict the dynamic particle movement, erosion rate and erosion location. However,

several restitution coefficients have been suggested to describe the effect of restitution coefficient and particle rebound behaviour [11]-[13]. In this study, three models are used which are derived experimentally, Forder et al. [13] particle-wall rebound model, Grant and Tabakoff [11] particle-wall rebound model and Sommerfeld and Huber [12] restitution coefficient model with the erosion prediction models to track particles and predict erosion. The restitution coefficients are divided into two elements namely, restitution coefficient in the normal direction e_n and restitution coefficient in the tangential direction e_t which represent change in particle velocity after impacting the wall. Forder et al. [13] suggested the following coefficient correlation for perpendicular and parallel velocity of the components for AISI 4130:

$$e_c = 0.988 - 0.78\alpha + 0.19\alpha^2 - 0.024\alpha^3 + 0.0027\alpha^4 \quad (17)$$

$$e_{par} = 1 - 0.78\alpha + 0.84\alpha^2 - 0.21\alpha^3 + 0.028\alpha^4 - 0.022\alpha^5 \quad (18)$$

where α is angle of particle incidence. Suggested model coefficient developed by Grant and Tabakoff [11] is as follows:

$$e_c = 0.993 - 1.76\alpha + 1.56\alpha^2 - 0.49\alpha^3 \quad (19)$$

$$e_{par} = 0.998 - 1.66\alpha + 2.11\alpha^2 - 0.67\alpha^3 \quad (20)$$

Sommerfeld and Huber [12] suggested a model for the normal restitution of coefficient. The relationship for normal coefficient of restitution is as follows:

$$e_c = \max(1 - 0.013\alpha, 0.7) \quad (21)$$

IV. Erosion Model

In predicting erosion in an elbow, several factors need to be considered such as impact angle and impact speed, particle size and shapes. These are considered as the factors causing erosion damage on the geometry of the elbow. Using these factors, the rate of erosion is then calculated. The rate of erosion can be described as mass loss of pipe wall by erosion divided by mass of impinging particle on the wall. Consequently, erosion rate is dependent on the particle impact angle and impact velocity and mass flow rate. However, in this work the generic model is used to calculate the erosion rate in the 90° elbow and the model is embedded in Ansys fluent given as follows:

$$ER = \Sigma_{p=1}^{Ntraj} \frac{m_p C(d_p) f(\alpha) v_p^n}{A_f} \quad (22)$$

where C stands for the material wall constant, n stands for the particle shape, which is considered with exponent values of 0.2, 0.53 and 1 for semi-rounded, rounded, and sharp particles, respectively. V_p stands for the impact velocity and $f(\alpha)$ stands for the impact angle function. Impact velocity exponent is an empirical constant

$$f(\alpha) = \begin{cases} a\theta^2 + b\theta; & \theta \le \theta_0 \\ x\cos^2(\theta)\sin(w\theta) + y\sin^2\theta + z; & \theta > \theta_0 \end{cases} \quad (23)$$

V. CFD Modelling

A. Description of Test Case

A commercial software was adopted (Ansys Fluent) to perform a numerical simulation. The data of the experiment carried out by [8] are employed in this study to examine the performed erosion models. The adopted experiment in [8] examined the erosion rate of long radius elbows of a pneumatic transport system. A 90-degree elbow was used as test piece with 25.4 mm diameter and a curvature radius of 38.1 mm, connected to a straight pipe length connecting upstream and downstream to an elbow were evaluated for a better way of representing the flow at the test specimen location. The simulation was run trying to replicate the same conditions as the one under which the experiment was done, see Table I. Consequently, in this study, a 20D = 810 mm vertical pipe upstream and a 10D = 410 mm horizontal pipe downstream of the elbow were used, which can be seen in Fig. 1.

TABLE I
Summary of Flow Conditions in [8]

Names	Value
Fluid	Air
Velocity	25.24 m/s
Particle diameter	100 μm
Mass flow rate (Particles)	0.0286 kg/m^3
Density of Particles	2650 kg/s
Pipe Material density (Steel)	7800 kg /m^3
Brinell Hardness (BH) Material	120

TABLE II
Experimental Data in [8]

Fitting Type	Fluid	D (mm)	R/D	U $(m/s)^0$	$d_p(\mu m)$	m_p (kg/s)	ER (m/s)
Eyler	Air	41	3.25	25.24	100	0.0286	2.86E-08

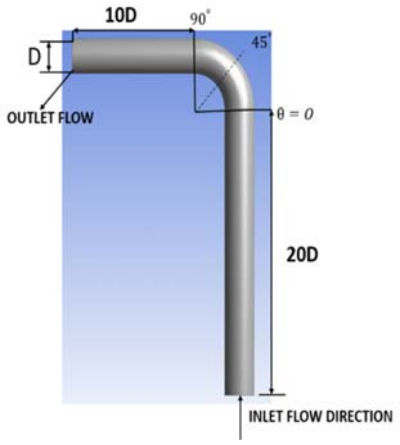

Fig. 1 Elbow geometry for simulation

B. Computational Mesh

A 3-D computational hexahedral structured mesh was adopted in this simulation. The mesh surface was generated carefully due to the significant effect on quality of resulting

mesh volume. A refinement near-wall region was done, in a high velocity gradients region and boundary layer was present. A structured hexahedral grid is used to mesh the surface of the cross-section, See fig 2. The grid number used in this case is approximately 12,60793.

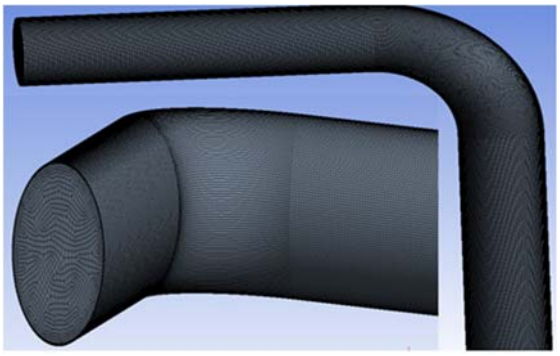

Fig. 2 Structure mesh use for simulation

C. Boundary Condition Parameters

Sand particles were injected uniformly at the inlet of the elbow at the same velocity as the fluid. The particles injected are spherical in shape. Parameter of roughness position is 0; that means the domain of the walls are smooth, and roughness constant is in the default value of 0.5. In addition, turbulence intensity position is 5%.

D. Numeric Method

Coupled procedures were used for velocity and pressure coupling. Discretization strategy was employed for pressure conditions and the second order discretization strategy was employed for divergence and convection conditions, also convergent benchmark used for calculations in the residual control volume for each of the equation is placed as 0.0001, energy equation is 10^{-6} and number of the iterations set is 2000 in a simulation of steady state. However, number of iterations for discrete phase model (DPM) is placed as 10.

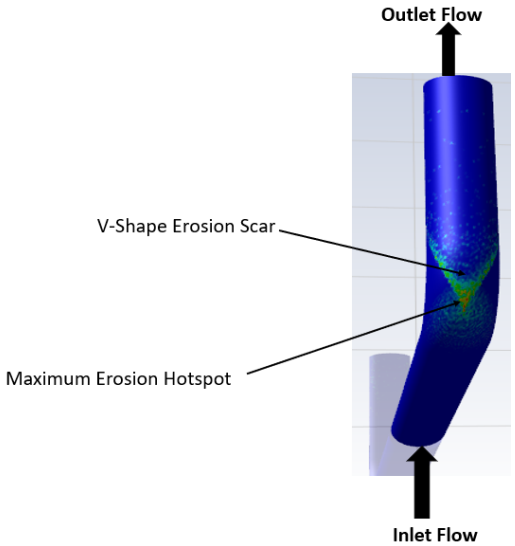

Fig. 3 Elbow Erosion Contour for simulation

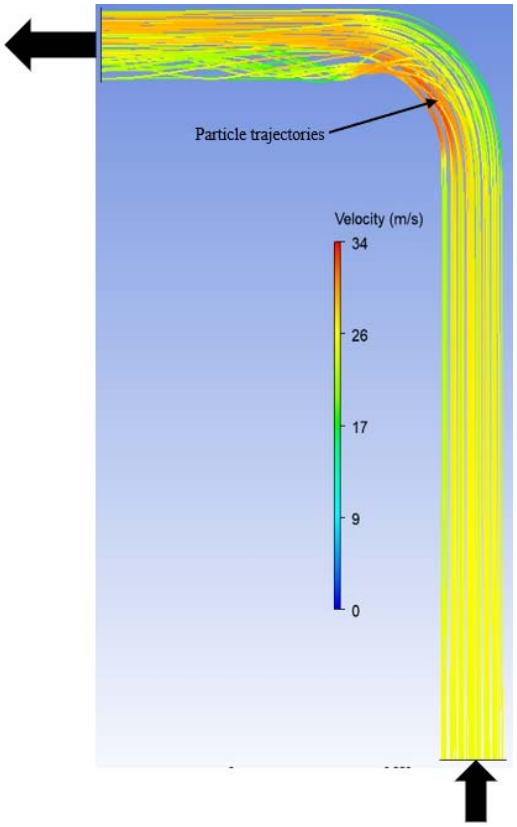

Fig. 4 Particle Trajectories

VI. Results and Discussion

In comparing the experimental data and predicted data in Tables II and III, the severity to erosion determination is characterized by the fluid characteristics, sand particle property and other essential parameters. Most erosion models define some few erosion rate calculation parameters, such as velocity of particles, size of particle, pipe materials, properties of fluid, etc. Impact angle function is one of the most critical parameters among the factors influencing erosion. Since most of the suggested impact angle functions are empirical and valid only for some defined situations, obtaining proper impact angle is important to predict accurate erosion rate. Therefore, the impact angle of the erosion models in Ansys Fluent and three restitution coefficient model were employed to track particles and predict erosion rate and compared with the experimental data to determine which is appropriate for this study. However, the generic solid particle erosion models used in the CFD prediction showed accurate predicted result. Fig. 3 shows erosion contour and Fig. 4 shows particle trajectories with the effect of velocity profile of the flow field in the elbows under the inlet velocity of 25.24 m/s and the CFD result in Table III shows the velocity impact angle effect due to the sand particles impinging on the wall of the elbow at high velocity and a point on the elbow were observed to have started turning red due to velocity increase and the maximum erosion locations occur at 48° which is in good agreement with the experimental data of [8].

TABLE III
PREDICTED DATA

g	D (mm)	R/D	$U_0(m/s)$	$d_p(\mu m)$	$m_p(kg/s)$	ER(m/s)
Air	50.8	1.5	25.24	100	0.0286	2.86E-08

VII. CONCLUSION

In this work, Euler-Lagrange with k–omega turbulent model is applied to treat the air and solid particle as continuous phases and the discrete phase was employed to simulate particles trajectories. Then, analysis was conducted on the effects imposed by flow velocity and impact of solid particles diameter, the elbow erosion rate was verified with experimental result in [8]. The conclusion is as follows:

1. The exponential increase of erosion rate is caused by the increase of flow velocity and for small size particles, erosion gravitate to occur inside the elbow wall under the influence of inferior flow and
2. For large particle size, the erosion gravitates to occur in the outer most part of elbow wall this is because of the inertial force acting on it.

ACKNOWLEDGMENT

The authors would like to acknowledge Petroleum Technology development fund and Energy and Power Theme, Cranfield University, Bedfordshire for supporting this study. The authors would also like to recognize supervisors Professor Nigel Simms and Dr Liyun Lao for their invaluable suggestions during the formation of this paper.

REFERENCES

[1] Lin, N., Lan, H., Xu, Y., Dong, S., and Barber, G., 2015, "Effect of the Gas-Solid Two-Phase Flow Velocity on Elbow Erosion," Journal of Natural Gas Science and Engineering, 26, pp. 581–586.
[2] Huang, C., Minev, P., Luo, J., and Nandakumar, K., 2010, "A Phenomenological Model for Erosion of Material in a Horizontal Slurry Pipeline Flow," Wear, 269(3–4), pp. 190–196.
[3] American Petroleum Institute, 1991, API Recommended Practice 14E Design and Installation of Offshore Production Platform Piping Systems.
[4] Tilly, G. P., 1979, "Erosion Caused by Impact of Solid Particles," 13, pp. 287–319.
[5] Salama, M. M., 2000, "An Alternative to Api 14e Erosional Velocity Limits for Sand-Laden Fluids," Journal of Energy Resources Technology, Transactions of the ASME, 122(2), pp. 71–77.
[6] Zhang, Y., Reuterfors, E. P., McLaury, B. S., Shirazi, S. A., and Rybicki, E. F., 2007, "Comparison of Computed and Measured Particle Velocities and Erosion in Water and Air Flows," Wear, 263(1-6 SPEC. ISS.), pp. 330–338.
[7] Chen, X., McLaury, B. S., and Shirazi, S. A., 2006, "A Comprehensive Procedure to Estimate Erosion in Elbows for Gas/Liquid/Sand Multiphase Flow," Journal of Energy Resources Technology, Transactions of the ASME, 128(1), pp. 70–78.
[8] Peng, W., and Cao, X., 2016, "Numerical Prediction of Erosion Distributions and Solid Particle Trajectories in Elbows for Gas-Solid Flow," Journal of Natural Gas Science and Engineering, 30, pp. 455–470.
[9] Faeth, G. M., 1986, "Spray Atomization and Combustion," AIAA, . 86-0136, pp. 1–17.
[10] Amsden, A., O'Rourke, P., and Butler, T., 1989, KIVA-II: A Computer Program for Chemically Reactive Flows with Sprays.
[11] Grant, G., and Tabakoff, W., 1975, "Erosion Prediction in Turbomachinery Resulting from Environmental Solid Particles," Journal of Aircraft, 12(5), pp. 471–478.
[12] Sommerfeld, M., and Huber, N., 1999, "Experimental Analysis of Modelling of Particle-Wall Collisions," International Journal of Multiphase Flow, 25(6–7), pp. 1457–1489.
[13] Forder, A., Thew, M., and Harrison, D., 1998, "A Numerical Investigation of Solid Particle Erosion Experienced within Oilfield Control Valves," Wear, 216(2), pp. 184–193.

Christopher Deekia Nwimae is a PhD researcher in Energy and Power, School of Water, Energy and Environment, Cranfield University, UK working on prediction and monitoring for subsea valve reliability and integrity management. He completed an MSc. in Offshore and Ocean Technology (Subsea Engineering) from Cranfield University, UK in 2016, with a thesis on potential corrosion issues in CO_2 pipelines. He has an undergraduate degree in mechanical engineering.

Christopher has over seven years industrial experience in welding and fabrication, corrosion monitoring and mitigation, pipeline pigging and maintenance, and valve maintenance and pressure testing.

Christopher is a student member of the following professional bodies: NICE, SPE, ASME, SUT.

Areas of Expertise: Erosion | Corrosion Prediction, Monitoring and Mitigation, Computational Fluid Dynamics (CFD), Risk and Reliability Engineering, Condition Monitoring, Material Selection, and Multiphase Flow.